

FUNDAMENTAL STUDY OF CRACK PROPAGATION OF EXTERNAL SULFATE ATTACK WITH MESOSCALE ANALYSIS SYSTEM FOR COUPLED CHEMO-MECHANICAL BEHAVIOURS

T. MIURA^{*}, Y. YAMAMOTO[†] AND H. NAKAMURA^{††}

^{*}Nagoya University

Nagoya, JAPAN

e-mail: t.miura@civil.nagoya-u.ac.jp

[†]Nagoya University

Nagoya, JAPAN

e-mail: y.yamamoto@civil.nagoya-u.ac.jp

^{††}Nagoya University

Nagoya, JAPAN

e-mail: hikaru@nagoya-u.jp

Key words: Sulfate attack, Cement hydration model, Sulfate attack analysis, RBSM, Expansion crack

Abstract: In this study, three dimensional numerical analysis systems, which can consider the change in physico- chemical property and expansive strain due to external sulfate attack, was constructed in order to evaluate the process of expansion cracking behavior. This analysis was coupled with cement hydration model, sulfate attack analysis and Rigid Body Spring Model. In this paper, this analysis was conducted to evaluate the expansive crack propagation in association with cement source and mix proportion. As results, it was confirmed that this analysis can describe signature expansion cracking behavior.

1 INTRODUCTION

It is known that sewage line and concrete structures constructed in hot spring could be affected by sulfate and sulfuric acid and their performance could dramatically decrease. Sulfate attack can make cement matrix fragile material and occur expansion crack due to precipitations such as gypsum and ettringite. Chemical degradations such as sulfate attack have strong relationship with environmental condition such as temperature, pH, concentration of sulfate ions and so on [1, 2].

As cementitious materials will be damaged by sulfate attack, it could influence to not only durability performance but also structural

performance. For example, when crack occurs due to external force such as soil pressure, sulfate ions can go through the crack and diffusivity of sulfate ions should become fast. In addition, weakening of cement matrix and expansion crack affects mechanical characteristics. Namely, considering prediction of performance of concrete structure deteriorated by sulfate attack, it is necessary to evaluate the mutual relationships between durability performance and structural performance.

In previous study, some researchers [3-6] tried to describe expansion crack due to sulfate attack by means of modeling of reaction of

sulfate ions and cement hydrates and numerical analysis considering transformation of cement matrix and expansive pressure. However, these methods could still not describe the change of degradation forms due to environmental condition, cement source, mix proportion, curing time and so on. In order to evaluate and predict the change in structural performance due to sulfate attack in association with these influential factors, highly developed numerical analysis is demanded.

In this study, coupled analysis, which was modeled by cement hydration model, sulfate attack analysis and crack propagation analysis, was developed so as to describe expansion cracking propagation in association with the difference of cement source and mix proportion and the adequacy of this analysis was validated based on previous experiment.

2 ANALYTICAL CONCEPT OF EXTERNAL SULFATE ATTACK

When expansion crack due to external sulfate attack will be tried to describe with numerical analysis, we should consider ion transfer, chemical reaction with cement hydrates, expansive pressure and expansion cracking propagation. In addition, if the effects of environmental condition, cement source, mix proportion are tried to evaluate, numerical

analysis should be able to consider the difference of outer solution such as pH and concentration of sulfate ion, precipitation and the change in physico-chemical properties on cementitious material along with hydration.

The analytical flow was shown in Fig.1. This analysis was composed by three analyses, which were cement hydration model, sulfate attack analysis and Rigid Body Spring Model (RBSM) [7]. These analyses were explained as below.

2.1 Cement hydration model

When cement matrix damaged by sulfate attack, sulfate ions react with calcium hydroxide (CH) and gypsum can produce. In highly pH solution, gypsum can dissolve in pore solution and ettringite which could have expansibility can produce by the reaction with monosulfate [1]. In addition, if the influences of cement source, mix proportion and curing time are tried to consider, cement hydration model should be introduced. In this analysis, based on Jennings's study [8], cement hydration model was easily constructed. In particular, mineral composition of clinker was estimated by chemical composition using Bogue's model [9]. Next, using Eq.1, hydration degree of each mineral composition was calculated along with curing time and the

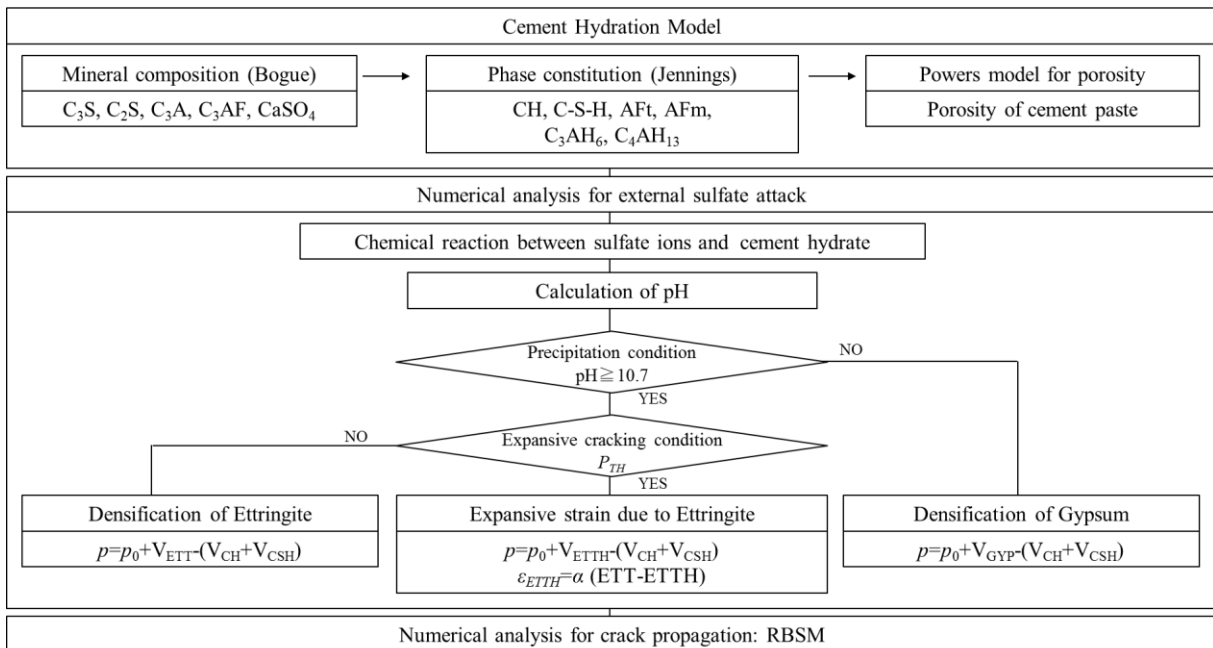


Figure 1: Analytical flow.

amount of cement hydrates such as CH, C-S-H, monosulfate, ettringite and so on were calculated by Jennings's model [8]. Furthermore, porosity of cement paste was calculated by Powers' model [10] as shown in Eq.2.

$$\alpha = 1 - \exp\left[-\left\{a_i(t-b_i)^{c_i}\right\}\right] \quad (1)$$

$$p = \frac{W/C - 0.36 \cdot \alpha}{W/C + 0.32} \quad (2)$$

where, α : hydration degree, i : kind of crincker, a_i , b_i , c_i : experiment constant, t : curing time (day), p : porosity in cement paste (cm^3/cm^3), W/C : water to cement ratio, respectively.

Then, following approaches were conducted to convert the amount of cement hydrates and porosity of cement paste into that of mortar. Firstly, total volume of fine aggregate was calculated by mix proportion and the volume of aggregates whose diameter are 1, 2, 3, 4, 5 mm was also calculated based on aggregate size distribution. Then, we can calculate the number of aggregate of each aggregate diameter. Furthermore, to convert porosity of cement paste into that of mortar, the volume of interaction transition zone (ITZ) was calculated as follows. As it was assumed that the length of ITZ was $3\mu\text{m}$, the total volume of ITZ can be calculated from the number of aggregate in association with aggregate diameter. Finally, porosity of mortar was calculated by porosity of cement paste, total volume of ITZ, volume of aggregate and volume of mortar. In addition, the other physico-chemical properties of mortar were derived as well as porosity.

2.2 Sulfate attack analysis

Sulfate attack analysis proposed by author [11] was modeled by ion transfer and chemical reaction. This analysis was discretized by finite volume method. In this analysis, expansive strain was calculated as initial strain in association with the amount of ettringite as discussed later. The main indexes of this analysis were explained as below.

(a) Sulfate ion transfer and reaction of cement hydrates

Sulfate ion transfer in liquid phase and reaction of cement hydrates in solid phase were described by Eq.3.

$$\frac{\partial(p \cdot C_{liquid})}{\partial t} = \frac{\partial}{\partial x} \left(D \frac{\partial(p \cdot C_{liquid})}{\partial x} \right) + \frac{\partial C_{solid}}{\partial t} \quad (3)$$

where, C_{liquid} : concentration of sulfate ion in liquid phase (mol/l), C_{solid} : concentration of sulfate ion in solid phase (mol/l), p : porosity of cement paste (cm^3/cm^3), D : diffusion coefficient of sulfate ion (mm^2/sec), respectively.

Based on Bentz's study [12], the influence of the change in pore structure was introduced by Eqs.4-5.

$$D = P_{vol} \cdot f(p) \cdot D_0 \quad (4)$$

$$f(p) = 0.001 + 0.07 \cdot p^2 + 1.7 \cdot H(p - 0.18)^2 \quad (5)$$

where, D_0 : the diffusion coefficient of sulfate ion in dilute solution (mm^2/sec), P_{vol} : the coefficient factor of the amount of cement paste, $f(p)$: pore structure function, $H(x)$: Heaviside function (if $x > 0$, $H(x) = 1$, if $x \leq 0$, $H(x) = 0$), respectively.

When expansive crack occurred, sulfate ion transfer should be accelerated in association with crack width. Idiart et al proposed model considering the effect of crack [3]. In this study, the acceleration of sulfate ion transfer was described based on Idiart's model as shown in Eqs.6-7. In fact, following model were modified because ion transfer can consider with one-dimensional element in this analysis.

$$D_w = D_0 \cdot w/w_c \quad (w \leq w_c) \quad (6)$$

$$D_w = D_0 \quad (w > w_c) \quad (7)$$

where, D_w : the diffusion coefficient of sulfate ion at the cracking area (mm^2/sec), w : crack width, w_c : critical crack width which was equal to 0.1 mm, respectively.

In this analysis, it was assumed that sulfate ions could react only CH. Then, sulfate ions can react CH linearly and the coefficient value of reaction rate of CH was introduced as shown in Eq.8. If experimental data was available, the coefficient value of K_{CH} was determined in association with the change in physico-chemical properties.

$$\frac{\partial C_{solid}}{\partial t} = -\sum (K_{CH} \cdot CH_{paste} \cdot C_{liquid}) \quad (8)$$

where, K_{CH} : the coefficient value of reaction rate of CH ($\text{cm}^3/\text{g}/\text{sec}$), CH_{paste} : the amount of CH in cement paste (g/cm^3), respectively.

(b) Precipitation condition

It is known that the precipitations such as gypsum and ettringite were influenced by the value of pH [13]. Then, in this analysis, precipitations condition was introduced by pH. In fact, the value of pH should be calculated by chemical equilibrium theory [14] which can be considered by equilibrium of ionic species. In this analysis, the change in pH in the pore solution was easily calculated by the change in CH as below.

$$pH = pH_{out} + (pH_{in} - pH_{out}) \cdot \frac{CH_{paste}}{CH_{paste0}} \quad (9)$$

where, pH_{out} : pH in the outer solution, pH_{in} : pH in the non-deteriorated area which value was 12.5, CH_{paste0} : initial amount of CH in cement paste (g/cm^3), respectively.

According to Gabrisova's research [13], ettringite can produce when the value of pH is more than 10.7 and gypsum can produce when the value of pH is less than 10.7 as shown in Fig.2. In addition, considering expansion crack due to ettringite, the reaction of monosulfate and gypsum should be focused [1] as shown in Fig.2. As the amount of Al_2O_3 in monosulfate calculated by cement hydration model, the limitation of producing ettringite was introduced in association with it. If it will be equal to zero, ettringite cannot produce.

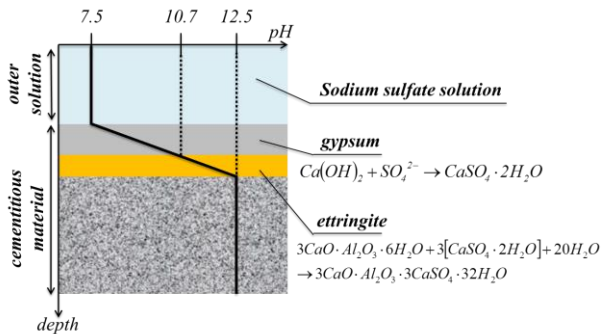


Figure 2: Precipitation condition using pH value and focused chemical reaction equations.

(c) Expansive pressure condition

In this study, it was assumed that only ettringite can contribute to expansion pressure although some researcher mentioned the contribution of gypsum [15]. According to previous study, it is known that expansive pressure shouldn't occur at once that ettringite produced in pore solution because ettringite should dissolve in pore solution at the initial reaction producing ettringite [15-18] as shown in Fig.3(a). When ettringite produces more than solution equilibrium, ettringite can produce in the pore as expansive pressure could occur gradually after that the crystal got into touch with pore wall as shown in Fig.3(b). However, the state of ettringite in the pore and how ettringite crystal pushes pore wall and makes expansive pressure are still not clear. Then, in this study, the threshold value p_{TH} which was derived by the ratio of porosity and initial porosity (p/p_0) was introduced in order to describe the mechanism of ettringite produce. When p/p_0 will be less than p_{TH} , expansive strain ϵ_{ETTH} can be introduced as shown in Eq.10. That is to say, the amount of ettringite produced, after that p/p_0 is less than p_{TH} , named effective ettringite can affect the expansive crack.

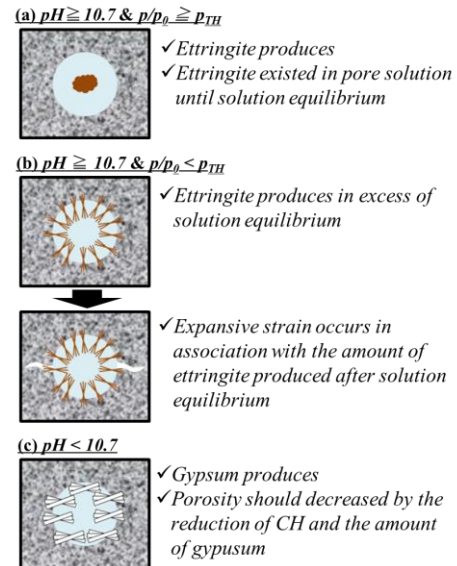


Figure 3: The concept of precipitations formation with expansive pressure condition, precipitation condition and calculation porosity. (a) and (b) were ettringite formation before and after expressive pressure and (c) was gypsum formation.

$$\varepsilon_{ETTH} = \alpha \cdot (ETT - ETTH) \quad (10)$$

where, ε_{ETTH} : expansive strain, α : the conversion factor of expansive strain (cm^3/g), ETT : the amount of ettringite in cement paste (g/cm^3), $ETTH$: the amount of ettringite in cement paste after p_{TH} (g/cm^3), respectively. Moreover, effective ettringite was derived by $ETT - ETTH$.

(d) Calculation of porosity

Porosity should be changed in association with the amount of precipitations and the reduction of CH. The calculation equations in the each condition were shown in Eqs.11-12.

$$p = p_0 + (V_{CH} - V_{ETT})/V \quad (pH \geq 10.7) \quad (11)$$

$$p = p_0 + (V_{CH} - V_{GYP})/V \quad (pH < 10.7) \quad (12)$$

where, V_{CH} : the volume increase due to the reduction of CH (cm^3/cm^3), V : the volume of each element, V_{ETT} , V_{GYP} : the volume reduction due to the amount of ettringite and gypsum (cm^3/cm^3), respectively.

As ettringite produced when pH is higher than 10.7, porosity was calculated by the reduction of CH and the amount of ettringite as shown in Eq.11. On the other hands, As gypsum produced when pH is lower than 10.7, porosity was calculated by the reduction of CH

and the amount of gypsum as shown in Eq.12 as shown in Fig.3(c). Thus, in this analysis, precipitation condition, expansive pressure condition and calculation of porosity were introduced so as to describe the complicated producing process of ettringite as shown in Fig.3.

2.3 Crack propagation analysis of RBSM

In this study, expansion cracking behavior was evaluated by three-dimensional RBSM [19]. RBSM is one of the discrete analyses [7, 20]. Fig.4 shows the voronoi particle definition of RBSM element. The element was solid made by random voronoi mesh and normal spring and two shear spring that numerical constitutive law was introduced were set into gauss points on the boundary surfaces in order to directly evaluate the crack propagation and crack width. Fig.5 shows the material models of mortar used in this analysis. Tensile model and shear models were set into normal springs and shear springs, where f_t is tensile strength, E is elastic modulus, G_f is tensile fracture energy, τ is shear strength, G is shear stiffness, f_c' is compressive strength. In fact, compression model of normal spring was modeled based on Yamamoto's model [19].

Expansive strain in association with effective

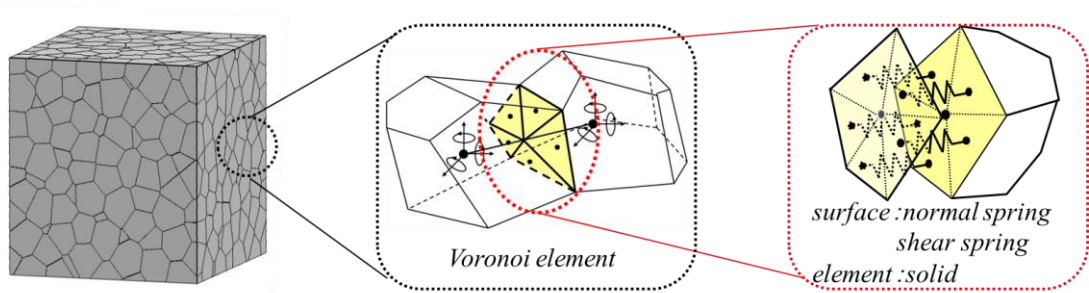


Figure 4: the voronoi particle definition of RBSM element.

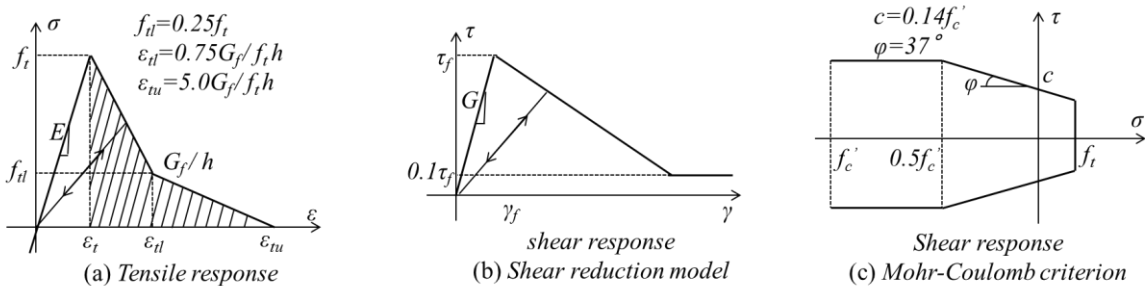


Figure 5: constitutive law of RBSM. (a), (b) and (c) are tensile response, shear reduction model and Mohr-Coulomb criterion, respectively.

ettringite was introduced to normal springs as initial strain. Then, it is known that when it damaged by sulfate attack, cement matrix could become fragile material and stress-strain relationship should be changed. In this study, it was, however, assumed that mechanical properties didn't change along with degradation.

2.4 Truss Network Model

The sulfate attack analysis was considered by Truss Network model [21] as shown in Fig.6. This model can describe ion transfer and chemical reaction of cement hydrates in the one dimensional truss elements where were set between the center of elements, the center of surface and the center of line constructing surfaces as shown in Fig.6. In this paper, these truss elements were named truss-1 and truss-2 as shown in Fig.6. In addition, the amount of physico-chemical properties such as cement hydrates, precipitations and porosity were contained in the volume of pyramid composed by center of element and boundary surface.

Before expansion cracking, ion transfer should occur at only truss-1 because the volume of truss-2 was equal to zero. After expansion crack, ions can move at not only truss-1 but also truss-2. In terms of truss-2, ion transfer can occur at cracking area calculated by crack width and the surface area. Then, the diffusion coefficient in cracking area was

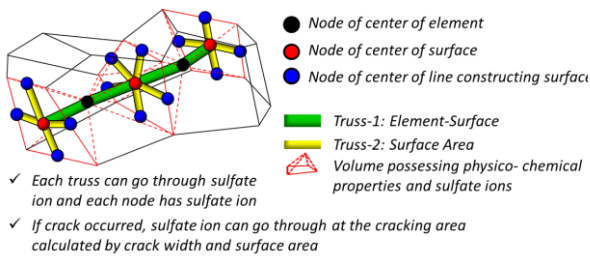


Figure 6: The overview of Truss Network Model.

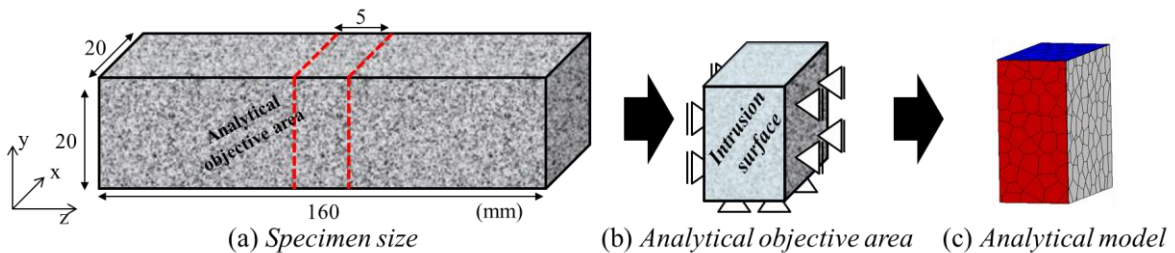


Figure 7: The overview of analytical objective. (a) shows specimen's size [22], (b) shows analytical objective area and (c) shows analytical model, respectively.

determined by Eqs.6-7 in association with crack width.

3 VALIDATION OF ANALYSIS

3.1 Overview of analytical objective

In this study, based on El-Hachem's experiment [22], the change of expansion crack propagation due to the kind of cement source and mix proportion were evaluated by this analysis.

Table 1: Mix proportion of El-Hachem's experiment

	W/C	W (kg/m ³)	C (kg/m ³)	S (kg/m ³)
M1	0.60	301	495	1409
M2	0.45	268	596	1409
M3	0.45	266	602	1409

The detail of analytical objective were shown in Fig.7 and Table.1. In El-Hachem's experiment, mortars were immersed in sodium sulfate solution in which concentration of sulfate ion and pH were 3g/l and 7.5, respectively. There were three kinds of mix proportion. The difference of M1 and M2 was W/C and mix proportion of M3 was same as M2 but, in case of M3, sulfate resistance cement was used. In this analysis, the curing time was set to 28 days. The size of mortar was 20×20×160mm as shown in Fig.7(a). In this analysis, the objective area was center of mortar in which size was 20×20×5mm and intrusion surface were set to X and Y-direction as shown in Fig.7(b). In addition, the surfaces of Z-direction were fixed so as not to deform and the bottom surface was fixed all direction. In addition, analytical model was constructed by using voronoi diagram whose averageing element size was 1.5 mm.

Table 2: The result of cement hydration model [22]

chemical composition (g/cm ³)			mineral composition (g/cm ³)				physico-chemical property				
M1	M2	M3	M1	M2	M3	M1	M2	M3			
<i>ref.</i>	<i>calc.</i>		<i>ref.</i>	<i>calc.</i>	<i>ref.</i>	<i>calc.</i>	<i>calc.</i>	<i>calc.</i>			
CaO	65.4	65.9	C ₃ S	66.4	65.2	67.5	67.5	CH (g/cm ³)	0.0493	0.0588	0.0559
SiO ₂	20.4	21.3	C ₂ S	5.6	9.3	6.7	10.2	C-S-H (g/cm ³)	0.106	0.1270	0.1320
Al ₂ O ₃	4.9	3.7	C ₃ A	11.4	9.9	2.2	2.2	Al ₂ O ₃ in AFm (g/cm ³)	0.0151	0.0179	0.0000
Fe ₂ O ₃	1.8	4.5	C ₄ AF	5.4	5.5	13.8	13.7	porosity (cm ³ /cm ³) <i>calc.</i>	0.190	0.150	0.150
SO ₃	3.6	2.6	CaSO ₄	—	6.1	—	4.4	porosity (cm ³ /cm ³) <i>ref.</i>	0.20	0.17	0.17

The results of cement hydration model were shown in Table.2. According to these results, the calculated mineral composition and porosity were a little bit different from experimental values. Calculated C₂S and calculated porosity were smaller than experiment one. However, the amount of cement hydrates and porosity were changed in association with the kind of mix proportion and cement source. In particular, in case of M3, the tendency of sulfate resistance cement was described because the amount of Al₂O₃ was equal to zero. For this reason, this cement hydration model can easily clarify the difference of mix proportion and cement source.

3.2 The evaluation of change in physico-chemical properties and expansive crack behavior

The coefficient factors which can influence to the distribution of ettringite and gypsum and expansion crack behavior were detected with the experimental result of the case of M1 [22]. The coefficient factors were K_{CH} , p_{TH} and α . K_{CH} can control the reaction between sulfate ions and CH. it should affect the amount of ettringite and gypsum and the change in pH because these items were calculated by the reduction of CH. On the other hand, p_{TH} can influence to the occurrence time of expansion crack. In addition, α should influence to the damage degree due to expansion crack.

According to objective experiment [22], after 106 days immersion, gypsum produced form surface to 1.5 mm and ettringite also produced from 1.5 mm to 2.5 mm in case of M1. The variety of precipitations should be controlled by K_{CH} . Firstly, the value of K_{CH} was detected with the experimental distribution of precipitations. Next, p_{TH} and α were detected by the cracking distribution in case of M1. According to the parametric analysis, The coefficient factors of K_{CH} , p_{TH} and α were calculated and these value were 0.01, 0.9 and 5×10^{-4} , respectively. In addition, mechanical properties of experiment and analysis introduced RBSM were shown in Table. 3. f_c^* and f_t^* were experimental compression strength and tensile strength [22]. E^* and G_f^* were estimated elastic modulus and .fracture energy based on JSCE standard [23].

The distribution of gypsum, ettringite, effective ettringite, porosity and porosity including cracking area at the cross section area in all cases after 100, 200 and 300 days immersion were shown in Fig.8. In fact, porosity including cracking area was calculated by porosity, crack width and cracking surface area.

As seen the distribution of gypsum, ettringite and porosity in case of M1 and M2, it was found that gypsum produced near the surface and ettringite also produced inner area of gypsum along with the reduction of CH and porosity changed along with the change in CH,

Table 3: Mechanical properties

	Experiment [22]		Constitutive laws of meso-scopic analysis				
	f_c^{*}	f_t^{*}	f_c' (MPa)	f_t (MPa)	E (GPa)	G_f (N/m)	c (MPa)
	(MPa)	(MPa)	$1.5f_c^{*}$	$0.8f_t^{*}$	$1.4E^{*}$	$0.5G_f^{*}$	$0.14f_c^{*}$
M1	56	7.9	84.0	6.32	47.9	0.0327	7.84
M2	77.5	10.1	116.3	8.08	52.9	0.0365	10.85
M3	82	10.2	123.0	8.16	53.5	0.0371	11.48

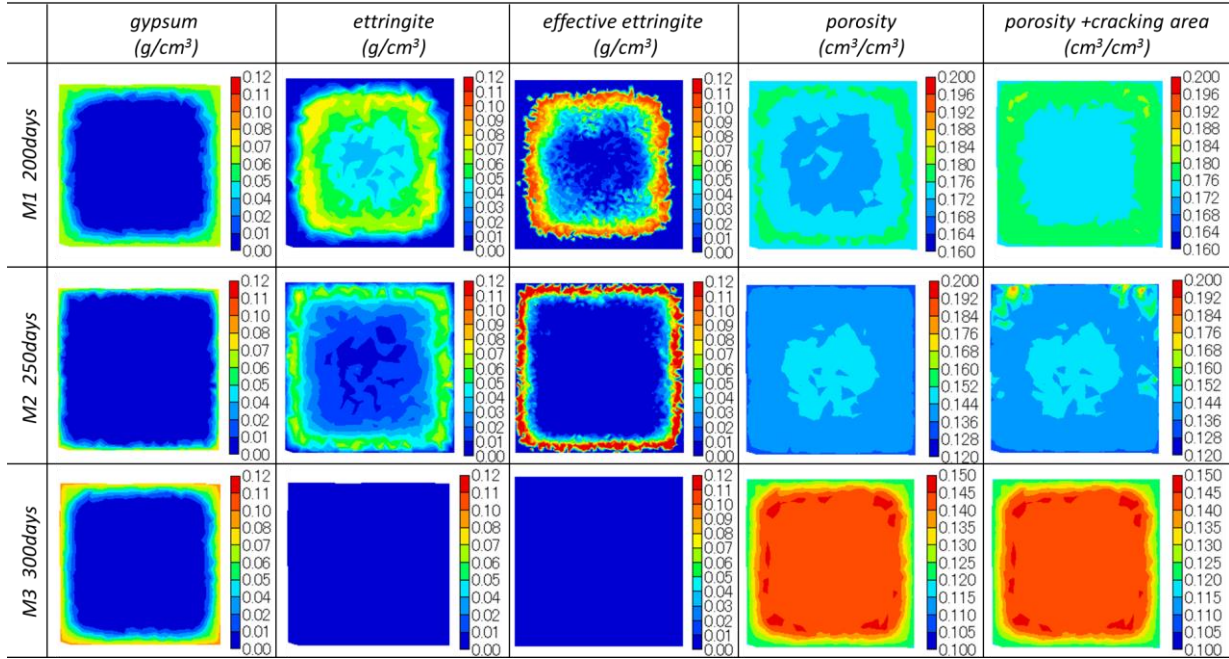


Figure 8: The distribution of gypsum, ettringite, effective ettringite, porosity and porosity including cracking area in all cases. The immersion time of these analytical results were different because cracking distribution shows difference immersion time in El-Hachem’s experiment [22].

gypsum, ettringite and expansion crack. The amount of ettringite was higher in case of M2 than M1 because of the difference of initial amount of Al_2O_3 . However, both cases had almost same tendency of the distribution of physico-chemical properties. As seen in distribution of effective ettringite and porosity including cracking area, it was found that porosity increased near the surface area and, at the almost same location, effective ettringite produced. On the other hands, in case of M3, there were no ettringite because initial Al_2O_3 was zero. That is why, porosity changed simply along with time due to reduction of CH and increment of gypsum.

Then, the deformation diagram in all cases after 100, 200 and 250 days immersion were shown in Fig.9. In case of M1 and M2, expansion crack didn’t appear after 100 days. After 200 and 250 days immersion, expansion

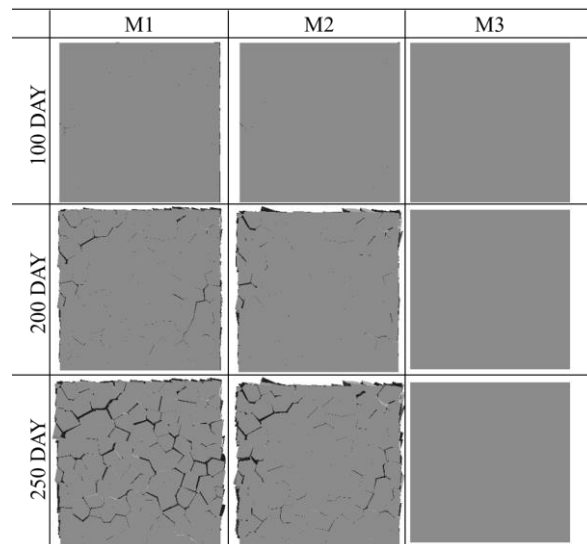


Figure 9: The deformation diagram after 100, 200 and 250 days immersion in all cases.

crack can be seen at near the surface area and the crack width at the inner area were bigger

than surface area. In particular, the damage degree of M1 was higher than M2 at the same immersion time and the occurrence of expansive crack in case of M1 was earlier than M2. This is because mechanical properties such as tensile strength of M1 was lower than M2 and the initial amount of Al₂O₃ in case of M1 was lower than M2. That is why, expansive crack easily occurred comparatively. Furthermore, in case of M3, the expansive crack didn't occur because ettringite couldn't produce as shown in Fig.9. These tendency were similar to experimental results [22].

4 DISCUSSION

Expansive crack due to external sulfate attack was quite complicated phenomena. One is that expansive crack due to ettringite occurs inner area concentrically and it doesn't appear at the surface [22, 24-25]. Another one is that expansion crack is strongly influenced by internal factors and external factors. Internal factors are mix proportion and cement source which can change the mechanical properties and physico-chemical properties. External factors are environmental conditions such as pH, sulfate ion, temperature and so on. When the expansive crack behavior is tried to describe, these indexes should be considered by numerical analysis, for example these reference [3-6].

In this paper, based on previous study, precipitation condition, expansive cracking condition with p_{TH} , expansive strain and the acceleration of ion transfer at the cracking area were introduced in order to describe expansive cracking behavior in association with the kind of cement source and mix proportion. This analysis can describe the signature tendency of external sulfate attack. In particular, expansive crack approximately occurred inner area concentrically as introducing expansive cracking condition, however, the crack also occurred near the surface. As describing the these tendency of expansive crack, the effective pore diameter which can be acted expansive pressure or mechanical behaviors changed by transformation of cement matrix should be considered.

As it now stands, the mechanism of expansive crack due to external sulfate attack is not clarified because it is difficult to determine the expansive pressure directly and to evaluate the change in mechanical behaviors due to the transformation of cement matrix. Hereafter, it is necessary to comprehend the mechanism of expansive cracking behavior with experimental and analytical approaches.

5 CONCLUSIONS

1. In this paper, numerical analysis coupled with cement hydration model, sulfate attack analysis and RBSM was developed to describe and evaluate the expansion cracking behavior due to external sulfate attack.
2. This analysis can evaluate that the difference of cement source and mix proportion affect distribution of physico-chemical properties and expansive crack behavior. These results were in good agreement with previous experiment. Finally, it was clarified that signature expansive cracking behavior can be described by this analysis.

ACKNOWLEDGMENT

Parts of this paper was funded by Grant-in Aid for Young scientists (B). The authors would like to thank the financial support.

REFERENCES

- [1] J. Skalny, J. Marchand, I. Odler 2002. Sulfate attack on concrete, *Modern Concrete Technology 10*.
- [2] A. Neville 2004. The confused world of sulfate attack on concrete, *Cement and Concrete Research*, Vol. 34, pp.1275-1296.
- [3] Andres E. Idiart, Carlos M. Lopez, I. Carol 2011. Chemo-mechanical analysis of concrete cracking and degradation due to external sulfate attack, *Cement and Concrete Research*, Vol.33, pp.411-423.
- [4] R. Tixier, B. Mobasher, M. ASCE 2003. Modeling of damage in cement-based materials subjected to external sulfate attack. II: Comparison with experiments, *Journal of Materials in Civil Engineering*,

- ASCE, Vol. 15, pp.314-322.
- [5] E. Samson, J. Marchand 2007. Modeling the transport of ions in unsaturated cement-based materials, *Computers and Structures*, Vol.85, pp.1740-1756.
- [6] S. Sarkar, S. Mahadevan, J.C.L. Meeussen, H. van der Sloot, D.S. Kosson 2010. Numerical simulation of cementitious materials degradation under external, *Cement and Concrete Composites*, Vol.32, pp.241-252.
- [7] T. Kawai 1978. New discrete models and their application to seismic response analysis of structure, *Nuclear Engineering and Design*, Vol.48, pp.207-229.
- [8] P. D. Tennis, H. M. Jennings 2000. A model for two types of calcium silicate hydrate in the microstructure of Portland cement pastes, *Cement and Concrete Research*, Vol.30, pp.855-863.
- [9] R. H. Bogue 1929. Calculation of compounds in Portland cements, *Industrial and Engineering Chemistry*, Analytical Edition 1, pp.192-197.
- [10] Powers T. C. 1960. Physical properties of cement paste, *Proceedings of 4th International Symposium on The Chemistry of Cement*, pp.577-613.
- [11] T. Miura, Y. Sato 2014. Numerical analysis for mortar deteriorated by sulfate acid attack considering influences of ettringite and gypsum, *Cement Science and Concrete Technology*, Vol.67, pp.216-223, 2014. (in Japanese)
- [12] E. Z. Garboczi, D. P. Bentz 1992. Computer simulation of the diffusivity of cement-based materials, *Journal of Materials Science*, Vol.27, pp.2083-2092.
- [13] A. Gabrisova, J. Havlica 1991. Stability of calcium sulphoaluminate hydrates in water solutions with various pH values, *Cement and Concrete Research*, Vol.21, pp.1023-pp.1027.
- [14] B. Johannesson, K. Yamada, L. O. Nilsson, Y. Hosokawa 2007. Multi-species ionic diffusion in concrete with account to interaction between ions in the pore solution and the cement hydrates, *Materials and Structures*, Vol.40, pp.651-665, 2007.
- [15] M.D. Cohen 1983. Modeling of expansive cements, *Cement and Concrete Research*, Vol.13, pp.519-528.
- [16] P.K. Mehta 1973. Mechanism of expansion associated with ettringite formation, *Cement and Concrete Research*, Vol.3, pp.1-6.
- [17] X. Ping, J.J. Beaudoin 1992. Mechanism of sulphate expansion I. Thermodynamic principle of crystallization pressure, *Cement and Concrete Research*, Vol. 22, pp.631-640.
- [18] J. Bizzozero, C. Gosselin, K. Scrivener 2014. Expansion mechanisms in calcium aluminate and sulfoaluminate, *Cement and Concrete Research*, Vol.56, pp.190-202.
- [19] Y. Yamamoto, H. Nakamura, I. Kuroda, N. Furuya 2014. Crack propagation analysis of reinforced concrete wall under cyclic loading using RBSM, *European Journal of Environmental and Civil Engineering*, Vol.18, No.7, pp.780-792.
- [20] J. Thomure, J. Bolander Jr., M. Kunieda 2001. Reducing mesh bias on fracture within rigid- body- spring networks, *Structural Eng./Earthquake Eng.*, JSCE, Vol. 18, No. 2, pp. 95-103.
- [21] H. Nakamura, W. Srisoros, R. Yashiro and M. Kunieda 2006. Time-Dependent Structural Analysis Considering Mass Transfer to Evaluate Deterioration Process of RC Structures, *Journal of Advanced Concrete Technology*, Vol.4, No.1, pp.147-158.
- [22] R. El-Hachem, E. Roziere, F. Grondin, A. Loukili 2012. Multi-criteria analysis of mechanism of degradation of Portland cement based mortars exposed to external sulphate attack, *Cement and Concrete Research*, Vol. 42, pp.1327-1335.
- [23] JSCE 2012. Standard specifications for concrete structures-Design. (in Japanese)
- [24] J. Bizzozero, C. Gosselin, K. Scrivener 2014. Expansion mechanisms in calcium aluminate and sulfoaluminate, *Cement and Concrete Research*, Vol.56, pp.190-202.
- [25] X. Ping, J.J. Beaudoin 1992. Mechanism of sulphate expansion II. Validation of thermodynamic theory, *Cement and Concrete Research*, Vol. 22, pp.845-854.